Paper

Estimation of UFMC Fading Channels Using H_∞ Filter

Ali Jamoos

Department of Electronic and Communication Engineering, Al-Quds University, Jerusalem, Palestine

https://doi.org/10.26636/jtit.2020.138819

Abstract—Universal filtered multi-carrier (UFMC) modulation is a very powerful candidate to be employed for future 5G mobile systems. It overcomes the limitations and restrictions in current modulation techniques employed in 4G mobile systems and supports future applications, such as machine-to-machine (M2M), device-to-device (D2D), and vehicle-to-vehicle (V2V) communications. In this paper, we address the estimation of UFMC fading channels based on the comb-type pilot arrangement in the frequency domain. The basic solution is to estimate the fading channel based on the mean square error (MSE) or least square (LS) criteria with adaptive implementation using least mean square (LMS) or recursive least square (RLS) algorithms. However, these adaptive filters seem not to be effective, as they cannot fully exploit fading channel statistics, particularly at high Doppler rates. To take advantage of these statistics, time-variations of the fading channel are modeled by an autoregressive process (AR), and are tracked by an H_∞ filter. This, however, requires that AR model parameters be known, which are estimated by solving the Yule-Walker equation (YWE), based on the Bessel autocorrelation function (ACF) of the fading channel with a known Doppler rate. Results of Matlab simulations show that the proposed H_∞ filter-based channel estimator is more effective when compared with existing estimators.

Keywords—5G, autoregressive model, channel estimation, fading channel, H_∞ filter, Kalman filter, LMS filter, RLS filter, UFMC.

1. Introduction

Orthogonal frequency division multiplexing (OFDM) is the current multiple access technique employed in modern communication systems, such as wireless local area networks (WLAN), power line communication (PLC), asymmetric digital subscriber lines (ADSL), digital audio broadcasting (DAB), and digital video broadcasting (DVB) [1], [2]. Simple transceiver design is a significant advantage of OFDM. Indeed, it uses the inverse fast Fourier transform (IFFT) at the transmitter and the fast Fourier transform (FFT) at the receiver [3], [4]. Nevertheless, it suffers from numerous shortcomings and limitations, such as the overhead of inserting the cyclic prefix (CP), high sensitivity to carrier frequency offset (CFO), and high peak average power ratio (PAPR) [5], [6]. To overcome these drawbacks, filter bank multi-carrier (FBMC) modulation is suggested and compared with OFDM in [3]. The design of the FBMC system is similar to that of OFDM, as it is based on IFFT/FFT pair's process. In contrast, it uses groups of digital filters to increase spectral efficiency as compared with OFDM, particularly when it is integrated with offset quadrature amplitude modulation (OQAM). The digital filters are capable of overcoming interference between the neighboring subcarriers, reducing sensitivity to CFO, and increasing resistance to estimation error due to time/frequency shift by the elimination of side-lobes.

The key design features of future multicarrier modulation techniques include flexibility, versatility, scalability, and efficiency, as these qualities mean that a wide range of future applications may be served [7]–[10]. Several multiple access schemes have been recently suggested as candidates for 5G [11]–[13]. Among them are FBMC, generalized frequency division multiplexing (GFDM) [14], and universal filtered multi-carrier (UFMC) [15]. It is found that UFMC has better spectral efficiency than FBMC [16], [17]. In addition, unlike FBMC, UFMC offers simple implementation and backward compatibility, as well as integrity with OFDM. It is also easier to update a CP-OFDM system to UFMC, than it is the case with FBMC. Furthermore, its implementation is based on IFFT/FFT pairs combined with a prototype filter known as the Chebyshev window with Nyquist pulse shaping, which may minimize spectral leakage limitations of OFDM and FBMC. Therefore, UFMC combines the benefits of OFDM and FBMC systems [13] and avoids their shortcomings. Its operation is based on filtering successive sub-bands (a group of subcarriers). The existence of orthogonal carriers is not important, which means that better spectral efficiency and low latency are achieved. Thus, UFMC may support future 5G applications, such as IoT and D2D, which require a strict synchronous transition between the transmitter and the receiver [18], while V2V requires a signal that is less sensitive to CFO in order to achieve reliable communication between mobile nodes.

Fading channel estimation and equalization techniques are critical in wireless communication systems in order to recover transmitted symbols at the receiver side. Several UFMC system studies have examined the issue of channel estimation and equalization so far [19]–[21]. In contrast, numerous studies were adopted in regard to OFDM [22]–[25] and FBMC systems [26]–[29] and may be found in the literature. Channel estimation procedures in the

UFMC and FBMC/OQAM systems are not similar to the regular techniques used in the OFDM system, since channel frequency response values are real in OFDM and complex in FBMC and UFMC. In addition, the use of the sub-bands filtering process to reduce out-of-band emissions could yield different filter gains on different subcarriers for one UFMC symbol [30]. In [30], [31], the authors have proposed to estimate UFMC channels and show that the conventional pilot-aided channel estimation used in OFDM is efficient in UFMC. In [32], the authors investigated channel estimation in an UFMC system based on the comb-type pilot pattern, using various algorithms, such as LSLI, DFT and RMMSE.

Recently, in [33] the authors introduced the estimation of UFMC time-varying fading channels based on comb-type pilots using adaptive filters. Evolution of the channel fading process is modeled by an autoregressive model and tracked by the Kalman filter. Results of the simulation show that performance of the Kalman filter is better than that of least mean square (LMS) and recursive least square (RLS) filters. Nevertheless, the Kalman filter requires strict Gaussian assumptions on the state-space representation of the fading channel system. Indeed, the driving process and measurement noise must be independent white and Gaussian. To avoid these assumptions and any model uncertainties, the H_∞ filter may be employed [34]–[38].

In this paper, we readdress the estimation of UFMC time-varying fading channels based on comb-type pilot symbols. In particular, UFMC fading channels are modeled by an autoregressive process and tracked by an H_∞ filter, while the autoregressive parameters are estimated using the so-called Yule-Walker equations based on the Bessel autocorrelation function of the fading channel with a known Doppler rate. The structure of the paper is as follows. The UFMC transceiver is introduced in Section 2. Autoregressive modeling and estimation of the UFMC fading channels by using the H_∞ filter are described in Section 3. Simulation results are presented in Section 4. Finally, the conclusions are drawn in Section 5.

2. UFMC System Model

The UFMC system is built on filtering a set of sub-bands, instead of filtering the whole spectrum, as it is the case in OFDM, or a single carrier, as in FBMC. Therefore, the spectrum range in the UFMC system will be formed from successive sub-bands, as shown in Fig. 1 [39].

Table 1 shows a comparative study between three multicarrier modulation systems: OFDM, FBMC, and UFMC. It is clear that the UFMC system is more attractive than the other two systems.

Table 1
Comparison between OFDM, FBMC, and UFMC systems

Item	OFDM	FBMC	UFMC
PAPR	High	High	High
Overhead	High	Low	Low
Receiver complexity	Low	High	High
MIMO support	Yes	No	Yes
Short bursts	No	No	Yes
Fragmented spectrum	No	Yes	Yes

Figures 2 and 3 show UFMC transmitter and receiver models, respectively. The operation of UFMC is based on filtering a group of sub-bands, instead of filtering a single carrier or the entire band. In the UFMC system, the input has the form of a set of complex QAM symbols. These symbols are then serial-to-parallel converted and divided into B sub-bands, containing the K symbol each. Frequency domain symbols $\boldsymbol{S} = [\boldsymbol{S}_{1K}\ \boldsymbol{S}_{2K}\ \ldots\ \boldsymbol{S}_{BK}]$ are then converted to time domain symbols $\boldsymbol{X} = [\boldsymbol{x}_{1K}\ \boldsymbol{x}_{2K}\ \ldots\ \boldsymbol{x}_{BK}]$ by the IFFT blocks. Since the number of complex symbols in each sub-band is lower than that of IFFT points N, the rest of the

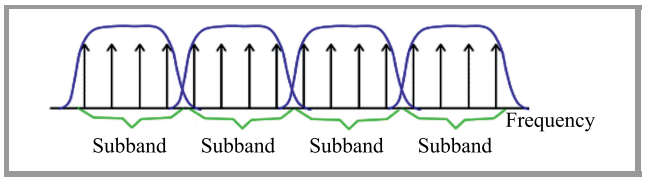

Fig. 1. UFMC signal in frequency domain.

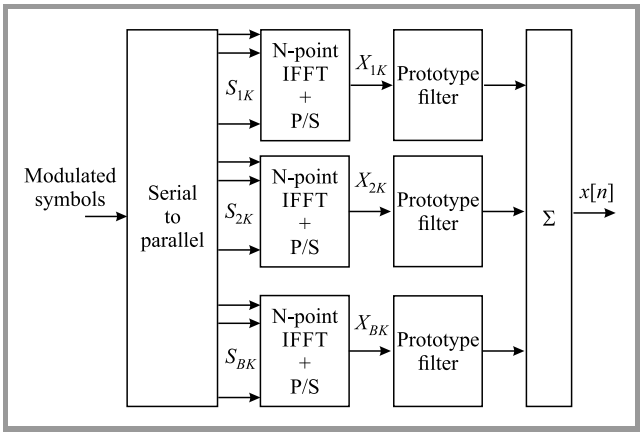

Fig. 2. UFMC transmitter block diagram.

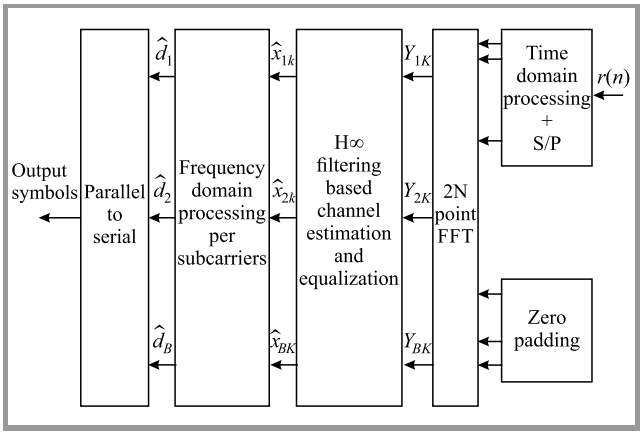

Fig. 3. UFMC receiver block diagram.

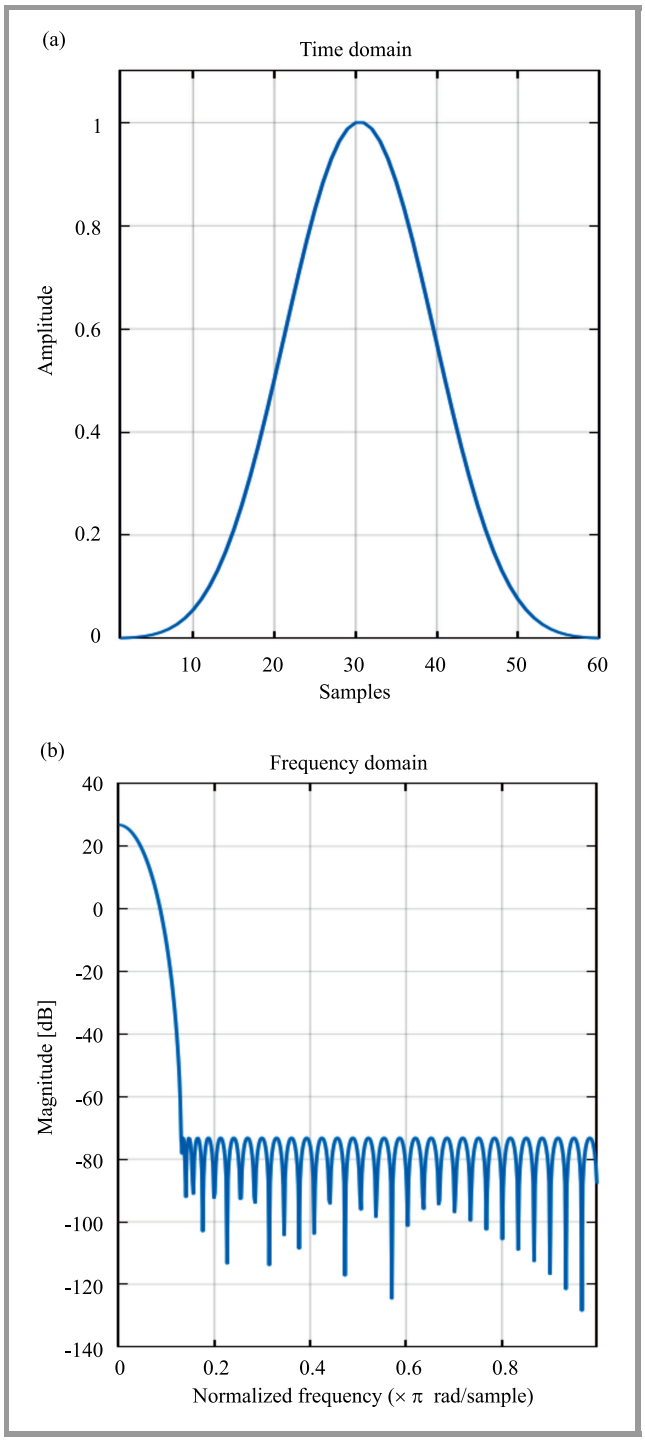

Fig. 4. Dolph-Chebyshev window in time and frequency domains for filter length $L = 60$.

block is padded with zeros. The output of IFFT is converted from parallel to serial. Each padded zero symbol is filtered with the Chebyshev finite impulse response (FIR) prototype filter with the length L, and a specific side lobe attenuation level. The Dolph-Chebyshev window had low side-lobe levels when compared with fixed window functions, such as the Hanning window. The Dolph-Chebyshev window in time and frequency domain for filter length of $L = 60$ is shown in Fig. 4. This will effectively decrease the out-of-band (OOB) emission. The output signals form each prototype filter are then added, and transmitted into the wireless channel. The transmitted UFMC signal may be expressed as [34]:

$$x(n) = \frac{1}{N}\sum_{i=1}^{B}\sum_{l=0}^{N+L-1}\sum_{k=1}^{K} s_{ik} e^{\frac{j2\pi kl}{N}} f(n-1) \ , \qquad (1)$$

where $f(n-l)$ denotes the Dolph-Chebyshev filter whose length is L.

UFMC has more elasticity for filtering every sub-band by its spectrum. It may allow the scheme to adapt service types by regulating sub-band and filter coefficients only. Indeed, UFMC may provide simultaneous access for two different applications, such as M2M and D2D, in two dissimilar sub-bands, without creating inter-symbol band interference (ISBI) due to the reduction of OOB [30].

3. H_∞ Filter-based Channel Estimation

The signal received from the time-varying frequency flat fading channel with additive white Gaussian noise (AWGN) over the k-th sub-carriers may be written as follows:

$$r_k(n) = x_k(n)h_k(n) + w_k(n) \ , \qquad (2)$$

where $x_k(n)$ is the transmitted UFMC signal over the k-th subcarriers, $w_k(n)$ denotes the AWGN process over the k-th subcarriers with the noise processes over all subcarriers being mutually independent and identically distributed (i.i.d.), each with zero-mean and variance σ_w^2. The time-varying flat fading process over the k-th subcarriers $h_k(n)$ is a complex Gaussian process $h_k(n) = |h_k(n)|e^{-j\varphi_k(n)}$ with a Rayleigh distributed envelope and a uniformly distributed phase.

The statistical characteristics of the fading channel $h_k(n)$ are described by its power spectrum density (PSD) and autocorrelation function (ACF). The PSD of the fading process is usually represented by the well-known U-shaped band limited Jakes spectrum with the maximum Doppler frequency f_d [40]:

$$\Psi_{hh}(f) = \begin{cases} \frac{1}{\pi f_d \sqrt{1-\left(\frac{f}{f_d}\right)^2}} \ , & \text{for} \quad f \le |f_d| \\ 0 \ , & \text{otherwise} \end{cases} \ , \qquad (3)$$

where $f_d = \frac{v}{\lambda}$ with v denotes the mobile speed and λ denotes the signal wavelength.

The corresponding discrete-time ACF is given by:

$$R_{hh}(m) = J_0\left(2\pi f_d T_s |m|\right) \ , \qquad (4)$$

where $J_0(.)$ denotes the zero-ordered Bessel function, T_s denotes the symbol period, and $f_d T_s$ is the Doppler rate.

To exploit the statistical properties of the fading channel given by its PSD – Eq. (3) and ACF – Eq. (4), the fading process over the k-th carrier is often approximated by

a p-th order AR process, denoted by AR(p) and defined as follows [41]:

$$h_k(n) = -\sum_{i=1}^{p} a_i h_k(n-i) + v_k(n) \ , \tag{5}$$

where $v_k(n)$ denotes the zero-mean complex white Gaussian driving process with equal variance σ_v^2 over all carriers and $\{a_i\}$ denotes the AR parameters.

To estimate the fading process $h_k(n)$ over the k-th carrier, and for the sake of simplicity and clarity of presentation, the carrier subscript is dropped. Let us define the state-vector as:

$$\boldsymbol{h}(n) = \begin{bmatrix} h(n) & h(n-1) & \dots & h(n-p+1) \end{bmatrix}^T \ . \tag{6}$$

Equations (5)–(6) may be written in the following state-space form:

$$\boldsymbol{h}(n) = \boldsymbol{\Phi}\boldsymbol{h}(n-1) + \boldsymbol{g}v(n) \ , \tag{7}$$

where $\boldsymbol{\Phi}$ denotes the state transition model matrix and may be expressed as follows:

$$\boldsymbol{\Phi} = \begin{bmatrix} -a_1 & -a_2 & \cdots & -a_p \\ 1 & 0 & \cdots & 0 \\ \vdots & \vdots & \ddots & \vdots \\ 0 & \cdots & 1 & 0 \end{bmatrix} \ , \quad \text{and} \quad \boldsymbol{g} = [1 \ 0 \ \dots \ 0]^T \ .$$

In addition, after dropping the carrier subscript, it follows from Eqs. (2) and (6) that:

$$r(n) = \boldsymbol{x}^T(n)\boldsymbol{h}(n) + w(n) \ , \tag{8}$$

where:

$$\boldsymbol{x}^T(n) = [x_{k,pilot} \ 0 \ \dots \ 0] \ , \tag{9}$$

with $x_{k,pilot}$ denoting the pilot symbols. Unlike Kalman filtering, H_∞ filtering not only deals with the estimation of the state vector $\boldsymbol{h}(n)$, but also makes it possible to focus on the estimation of a specific linear combination of the state vector components as:

$$z(n) = \boldsymbol{l}\boldsymbol{h}(n) \ , \tag{10}$$

where $\boldsymbol{l}$ denotes a linear transformation operator whose size is $1 \times p$. In order to estimate the fading process $\boldsymbol{h}(n)$, the linear operator is set to be $\boldsymbol{l} = \boldsymbol{g}^T = [1 \ 0 \ \dots \ 0]^T$.

Given the state space representation of the fading channel system by Eqs. (7), (8), and (10), H_∞ filtering may provide an estimation of the fading process $\hat{h}(n) = \boldsymbol{l}\hat{\boldsymbol{h}}(n)$ by minimizing the H_∞ norm of the transfer operator that maps the noises $w(n)$, $v(n)$, and the initial state error $\boldsymbol{e}_0 = \boldsymbol{h}(0) - \boldsymbol{h}(0)$ to the estimation error $e(n) = h(n) - \hat{h}(n)$, as follows:

$$J_\infty = \sup_{w(n), v(n), \boldsymbol{h}(n0)} J \ , \tag{11}$$

where:

$$J = \frac{\sum_{n=0}^{N-1} |e(n)|^2}{e_0^H \boldsymbol{P}_0^{-1} e_0 + \sum_{n=0}^{N-1} \left(Q_w^{-1} |w(n)|^2 + R_v^{-1} |v(n)|^2 \right)} \ , \tag{12}$$

with $\boldsymbol{P}_0$, $Q_w > 0$ and $R_v > 0$ being the weighting parameters adjusted by the designer to achieve the best performance needs and N denotes the number of data samples.

However, as a closed-form solution to the above optimal H_∞ estimation problem does not always exist, the following suboptimal design strategy is usually considered [37]:

$$J_\infty =< \gamma^2 \ , \tag{13}$$

where $\gamma > 0$ is a prescribed threshold of disturbance attenuation. Taking into account the approach introduced in [37], there exists an H_∞ channel estimator $\hat{h}(n)$ for a given $\gamma > 0$ if there exists a stabilizing symmetric positive definite solution $\boldsymbol{P}(n)$ to the following Riccati-type equation:

$$\boldsymbol{P}(n+1) = \boldsymbol{\Phi}\boldsymbol{P}(n)\boldsymbol{C}^{-1}(n)\boldsymbol{\Phi}^H + \boldsymbol{g}Q_w\boldsymbol{g}^T, \ \ \boldsymbol{P}(0) = \boldsymbol{P}_0 \ , \tag{14}$$

where:

$$\boldsymbol{C}(n) = \boldsymbol{I}_p - \gamma \boldsymbol{l}^T \boldsymbol{l}\boldsymbol{P}(n) + \boldsymbol{x}(n)R_v^{-1}\boldsymbol{x}^T(n)\boldsymbol{P}(n) \ . \tag{15}$$

This leads to the following constraint:

$$\boldsymbol{P}(n)\boldsymbol{C}^{-1}(n) > 0 \ . \tag{16}$$

If the condition (16) is satisfied, then the H_∞ channel estimator may be written as:

$$\hat{h}(n) = \boldsymbol{l}\hat{\boldsymbol{h}}(n) \ , \tag{17}$$

$$\hat{\boldsymbol{h}}(n) = \boldsymbol{\Phi}\hat{\boldsymbol{h}}(n-1) + \boldsymbol{K}(n)\alpha(n), \quad \hat{\boldsymbol{h}}(0) = \boldsymbol{0} \ , \tag{18}$$

where the so-called innovation process $\alpha(n)$ and the H_∞ estimator gain $\boldsymbol{K}(n)$, are given, respectively, by:

$$\alpha(n) = r(n) - \boldsymbol{x}^T(n)\boldsymbol{\Phi}\hat{\boldsymbol{h}}(n-1) \ , \tag{19}$$

$$\boldsymbol{K}(n) - \boldsymbol{P}(n)\boldsymbol{C}^{-1}(n)\boldsymbol{x}(n)R_v^{-1} \ . \tag{20}$$

It should be noted that the H_∞ channel estimator (14)–(20) has a similar observer structure as its Kalman counterpart. However, due to (15), the H_∞ channel estimator has a computational cost that is slightly higher than that of the Kalman solution. Indeed, if the weighting parameters $\boldsymbol{P}_0$, Q_w and R_v are chosen to be σ_w^2, σ_v^2, respectively, and the initial error covariance matrix is $\boldsymbol{h}(0)$, then as $\gamma \to \infty$ the H_∞ estimator is reduced to the Kalman estimator.

According to Fig. 2, the received signal $r_k(n)$ is first passed into the $2N$ point FFT block that transforms the time domain signal to the frequency domain. This is necessary for recovering symbols at N subcarriers from $N+L-1$ received signal samples. The result of the FFT block transformer is:

$$Y(k) = \frac{1}{\sqrt{N}} \sum_{l=0}^{N+L-2} r_k(n) \mathrm{e}^{\frac{-\mathrm{j}2\pi lk}{2N}}, \quad k = 0, 1, \dots, 2N-1 \ . \tag{21}$$

Once the fading channel $h_k(n)$ at pilot symbol location is estimated using the proposed H_∞ based channel estimator, channel equalization may be performed by multi-

plying Eq. (24) with a normalized version of the complex conjugate of the fading channel estimate $\hat{h}_k(n)$ as:

$$\hat{x}_k(n) = Y_k(n)\left(\frac{\hat{h}_k^*(n)}{|\hat{h}_k(n)|^2}\right). \tag{22}$$

4. Simulation Results

In this section, a comparative simulation study concerned with estimation of the UFMC fading channels is carried in connection with the proposed H_∞ based channel estimator and other channel estimators based on LMS, RLS and Kalman filters. Several interpolation techniques, such as linear interpolation, spline interpolation, and low-pass interpolation are investigated for estimating the fading channel at data symbol location. The fading channel is generated according to the AR model with the order of $p = 2$ [41]. The simulation parameters are summarized in Table 2.

Table 2
Simulation parameters

Modulation type	QAM modulation
Filter type	Dolph-Chebyshev with length $L = 60$
AR parameters	$a_1 = 1.96$, $a_2 = -0.99$
LMS step size	$\mu = 0.03$
RLS forgetting factor	$\lambda = 0.4$
Pilot ratio	1/8
Number of pilot symbols N_p	1024

Figure 5 shows the bit error rate performance of UFMC versus SNR with QAM. It is clear that the QAM modulation with bits-per-subcarrier of $M = 4$ results in the best BER performance.

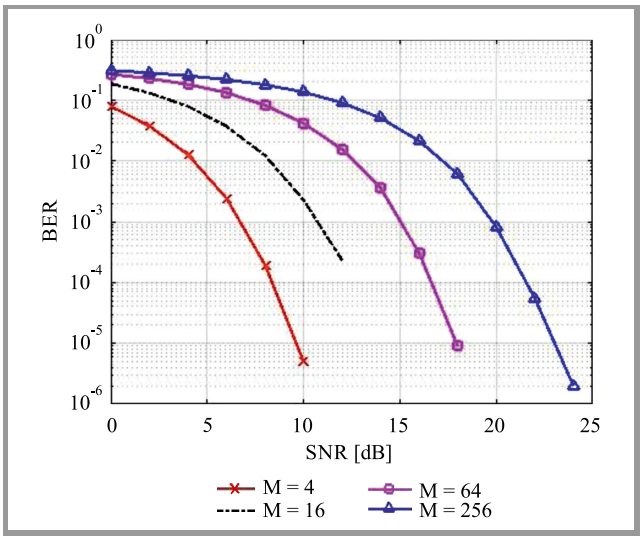

Fig. 5. BER versus SNR for UFMC with QAM modulation. (For color pictures see the electronic version of the paper.)

Figures 6–8 illustrate power spectrum density (PSD) with the same number of subcarriers (200 subcarriers) for UFMC, OFDM, and FBMC systems, respectively. It is clear that PSD of the UFMC system is more attractive than that of OFDM and FBMC.

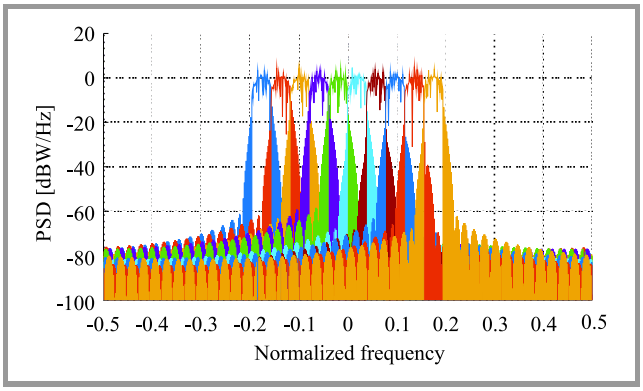

Fig. 6. PSD versus normalized frequency for UFMC system.

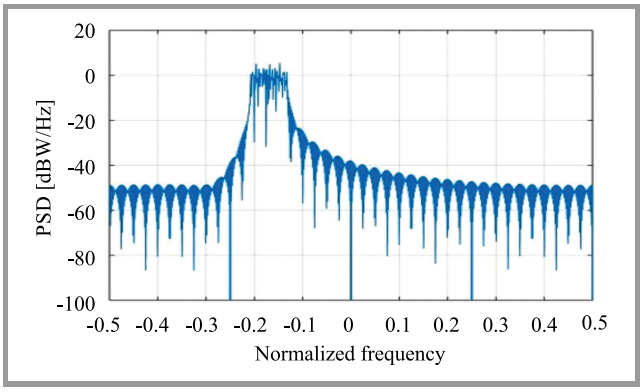

Fig. 7. PSD versus normalized frequency for OFDM system.

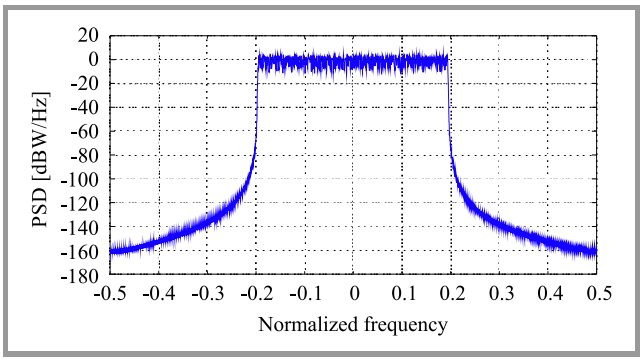

Fig. 8. PSD versus normalized frequency for FBMC system.

Figures 9 and 10 show the BER performance versus SNR for the UFMC system with two different values of Doppler rates $f_d T_s = 0.1111$ and $f_d T_s = 0.0741$, respectively. One may notice that the proposed H_∞ channel estimator yields the best BER performance, particularly at high Doppler rates. In addition, the LMS and RLS channels estimators fail to track the fading channel at high Doppler rates, which results in worse BER performance.

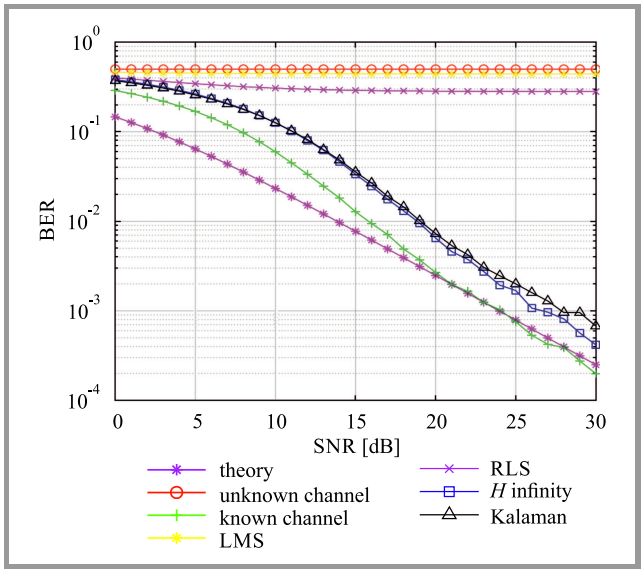

Fig. 9. BER vs. SNR for $f_d T_s = 0.1111$.

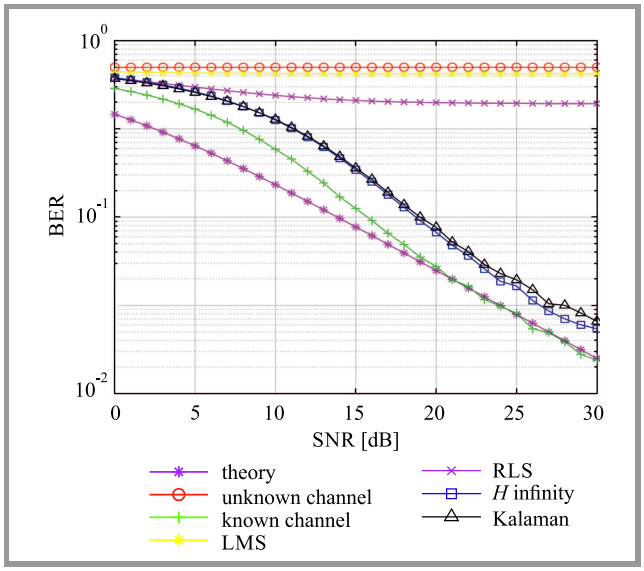

Fig. 10. BER vs. SNR for $f_d T_s = 0.0741$.

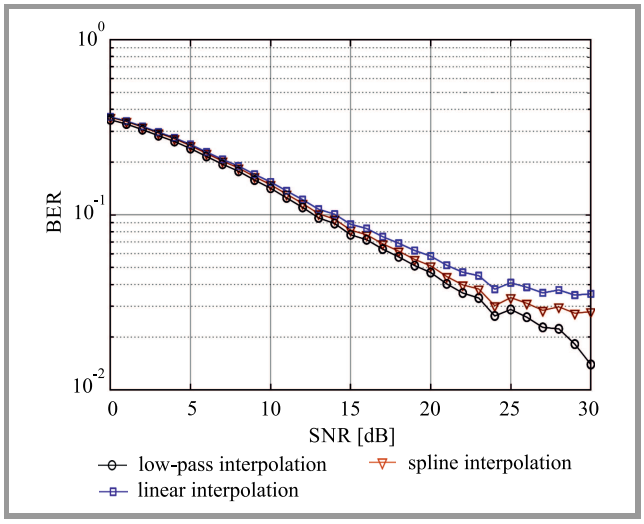

Fig. 11. BER vs. SNR with various interpolation techniques.

Figure 11 illustrates the BER performance of the UFMC system when employing the proposed H_∞ channel estimator with various interpolation methods for the Doppler rate of $f_d T_s = 0.0167$. It is confirmed that low-pass interpolation yields the best BER performance.

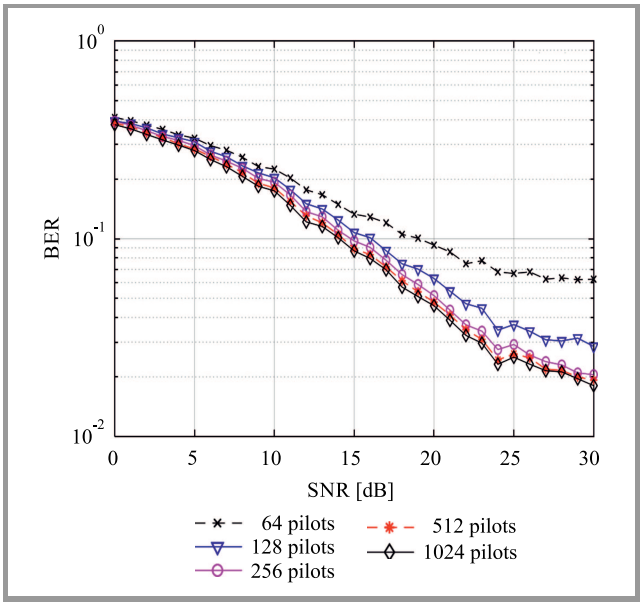

Fig. 12. BER vs. SNR with various pilot symbol values.

Figure 12 shows the effect that changing the number of pilot symbols N_p has on the BER performance of the UFMC system when using the proposed channel estimator with low-pass interpolation. Indeed, increasing the number of pilot symbols N_p will improve the BER performance of the system.

5. Conclusion

The UFMC system is a very strong candidate for the future generation of wireless applications. Indeed, it combines the advantages of both OFDM and FBMC and avoids their drawbacks. It achieves a higher data rate and higher spectral efficiency than other modulation systems. Furthermore, it solves the fixed synchronization problem experienced by current modulation systems and supports new applications, such as IoT, D2D, V2V, and M2M.

Estimation and equalization of UFMC fading channels based on the comb-type pilot symbol arrangement is addressed in this paper. The estimation process is carried-out in two stages. In the first stage, the fading channel at pilot carrier is estimated by using the H_∞ filter, the Kalman filter, the RLS algorithm, and the LMS algorithm. In the second stage, estimation of the fading channel at data symbol position is performed by using various interpolation techniques (linear, low-pass, and spline). Simulation results show that the proposed H_∞ filter-based channel estimator outperforms LMS, RLS, and Kalman estimators. In addition, the low-pass interpolation is confirmed to outperform both spline and linear interpolation.

References

[1] Y. G. Li and G. L. Stüber, Eds., *Orthogonal Frequency Division Multiplexing for Wireless Communications*. Springer, 2006 (ISBN 978-0-387-29095-9).

[2] K. K. Baum, B. Classon, and Ph. Sartori, *Principles of Broadband OFDM Cellular System Design*. Wiley, 2008 (ISBN: 9780470516379).

[3] B. Farhang-Boroujeny, "OFDM versus filter bank multicarrier", *IEEE Signal Process. Mag.*, vol. 28, no. 3, pp. 92–112, 2011 (DOI: 10.1109/MSP.2011.940267).

[4] H. H. Zhang, D. Le Ruyet, D. Roviras, Y. Medjahdi, and H. Sun, "Spectral efficiency comparison of OFDM/FBMC for uplink cognitive radio networks", *EURASIP J. on Adv. in Signal Process.*, Article no. 621808, 2010 (DOI: 10.1155/2010/621808).

[5] T. T. Lin and F. H. Hwang, "On the CFO/Channel estimation technique for MIMO-OFDM systems without using a prior knowledge of channel length", *EURASIP J. on Wirel. Commun. Network.*, Article no. 79, 2015 (DOI: 10.1186/s13638-015-0318-1).

[6] K. Anoh, C. Tanriover, B. Adebisi, and M. Hammoudeh, "A new approach to iterative clipping and filtering PAPR reduction scheme for OFDM systems", *IEEE Access*, vol. 6, pp. 17533–17544, 2018 (DOI: 10.1109/ACCESS.2017.2751620).

[7] F. Hu, *Opportunities in 5G Networks: A Research and Development Perspective*. Boca Raton, FL, USA: CRC Press, 2016 (ISBN: 9781498739542).

[8] Y. Liu *et al.*, "Waveform design for 5G networks: Analysis and comparison", *IEEE Access*, vol. 5, pp. 19282–19292, 2017 (DOI: 10.1109/ACCESS.2017.2664980).

[9] M. Addad and A. Djebbari, "Suitable spreading sequences for asynchronous MC-CDMA systems", *J. of Telecommun. and Inform. Technol.*, no. 3, pp. 9–13, 2018 (DOI: 10.26636/jtit.2018.118217).

[10] R. Nissel, S. Schwarz, and M. Rupp, "Filter bank multicarrier modulation schemes for future mobile communications", *IEEE J. Selec. Areas in Commun.*, vol. 35, no. 8, pp. 1768–1782, 2017 (DOI: 10.1109/JSAC.2017.2710022).

[11] G. Wunder *et al.*, "5GNOW: non-orthogonal, asynchronous waveforms for future mobile applications," *IEEE Commun. Mag.*, vol. 52, no. 2, pp. 97–105, 2014 (DOI: 10.1109/MCOM.2014.6736749).

[12] F. Schaich and T. Wild, "Waveform contenders for 5G-OFDM vs. FBMC vs. UFMC", in *Proc. of the IEEE Int. Symp. on Commun., Control and Sig. Process. ISCCSP 2014*, Athens, Greece, 2014, pp. 457–460 (DOI: 10.1109/ISCCSP.2014.6877912).

[13] R. Gerzaguet *et al.*, "The 5G candidate waveform race: a comparison of complexity and performance", *EURASIP J. on Wirel. Commun. and Network.*, Article no. 13, 2017 (DOI: 10.1186/s13638-016-0792-0).

[14] G. G. Fettweis, M. Krondorf, and S. Bittner, "GFDM-generalized frequency division multiplexing", in *Proc. IEEE 69th Veh. Technol. Conf. VTC Spring 2009*, Barcelona, Spain, 2009 (DOI: 10.1109/VETECS.2009.5073571).

[15] V. Vakilian, T. Wild, F. Schaich, S. ten Brink, and J.-F. Frigon, "Universal-filtered multi-carrier technique for wireless systems beyond LTE", in *Proc. IEEE Globecom Workshops GC Wkshps 2013*, Atlanta, GA, USA, 2013, pp. 223–228 (DOI: 10.1109/GLOCOMW.2013.6824990).

[16] F. F. Schaich, T. Wild, and Y. Chen, "Waveform contenders for 5G-suitability for short packet and low latency transmissions", in *Proc. IEEE 79th Veh. Technol. Conf. VTC Spring 2014*, Seoul, South Korea, 2014 (DOI: 10.1109/VTCSpring.2014.7023145).

[17] Y. Chen, T. Wild, and F. Schaich, "5G air interface design based on universal Filtered (UF-)OFDM", in *Proc. 19th Int. Conf. on Digit. Sig. Process.*, Hong Kong, China, 2014, pp. 699–704 (DOI: 10.1109/ICDSP.2014.6900754).

[18] G. Kongara, L. Yang, C. He, and J. Armstrong, "A comparison of CP-OFDM, PCC-OFDM and UFMC for 5G uplink communications", *IEEE Access*, vol. 7, pp. 157574–157594, 2019 (DOI: 10.1109/ACCESS.2019.2949792).

[19] X. Wang, T. Wild, F. Schaich, and S. ten Brink, "Pilot-aided channel estimation for universal filtered multi-carrier", in *Proc. IEEE Veh. Technol. Conf. VTC2015-Fall 2016*, Boston, MA, USA, 2015 (DOI: 10.1109/VTCFall.2015.7391089).

[20] K. Zerhouni, F. Elbahhar, R. Elassali, and K. Elbaamrani, "Performance of universal filtered multicarrier channel estimation with different pilots arrangements", in *Proc. IEEE 5G World Forum 5GWF 2018*, Silicon Valley, CA, USA, 2018, pp. 327–332 (DOI: 10.1109/5GWF.2018.8517030).

[21] R. Wang, J. Cai, X. Yu, and S. Duan, "Compressive channel estimation for universal filtered multi-carrier system in high-speed scenarios", *IET Commun.* vol. 11, no. 15, pp. 2274–2281, 2017 (DOI: 10.1049/iet-com.2017.0308).

[22] M. K. Ozdemir and H. Arslan, "Channel estimation for wireless OFDM systems", *IEEE Commun. Surv. & Tutor.*, vol. 9, no. 2, pp. 18–48, 2007 (DOI: 10.1109/COMST.2007.382406).

[23] Y. Liu, Z. Tan, H. Hu, L. J. Cimini, and Y. G. Li, "Channel estimation for OFDM", *IEEE Commun. Surv. & Tutor.*, vol. 16, no. 4, pp. 189–1908, 2014 (DOI: 10.1109/COMST.2014.2320074).

[24] S. Park, B. Shim, and J. Choi, "Iterative channel estimation using virtual pilot signals for MIMO-OFDM systems", *IEEE Trans. on Sig. Process.*, vol. 63, no. 12, pp. 3032–3045, 2015 (DOI: 10.1109/TSP.2015.2416684).

[25] J. Lin, "Least-squares channel estimation for mobile OFDM communication on time-varying frequency-selective fading channels", *IEEE Trans. on Veh. Technol.*, vol. 57, no. 6, pp. 3538–3550, 2008 (DOI: 10.1109/TVT.2008.919611).

[26] M. Aldababseh and A. Jamoos, "Estimation of FBMC/OQAM fading channels using dual Kalman filters", *The Scientific World J.*, Article no. 586403, pp. 1–9, 2014 (DOI: 10.1155/2014/586403).

[27] E. Kofidis, D. Katselis, A. Rontogiannis, and S. Theodoridis, "Preamble-based channel estimation in OFDM/OQAM systems: A review", *Signal Process.*, vol. 93, no. 7, pp. 2038–2054, 2013 (10.1016/j.sigpro.2013.01.013).

[28] O. E. Ijiga, O. O. Ogundile, A. D. Familua, and D. J. Versfeld, "Review of channel estimation for candidate waveforms of next generation networks", *Electronics*, vol. 8, no. 9, 2019 (DOI: 10.3390/electronics8090956).

[29] C.-W. Chen and F. Maehara, "An enhanced MMSE subchannel decision feedback equalizer with ICI suppression for FBMC/OQAM systems", in *Proc. Int. Conf. on Comput., Network. and Commun. ICNC 2017*, Santa Clara, CA, USA, 2017, pp. 1041–1045 (DOI: 10.1109/ICCNC.2017.7876278).

[30] L. Zhang, A. Ijaz, P. Xiao, M. A. Imran, and R. Tafazolli, "MU-UFMC system performance analysis and optimal filter length and zero padding length design" [Online]. Available: http://arxiv.org/pdf/1603.09169v1.pdf

[31] X. Wang, "Channel estimation and equalization for 5G wireless communication systems", Master Thesis, University of Stuttgart, 2014 [Online]. Available: https://www.researchgate.net/publication/273574825_Channel_Estimation_and_Equalization_for_5G_Wireless_Communication_Systems

[32] L. Zhang, C. He, J. Mao, A. Ijaz, and P. Xiao, "Channel estimation and optimal pilot signals for universal filtered multi-carrier (UFMC) systems", in *Proc. of the IEEE 28th Ann. Int. Symp. on Personal, Indoor, and Mob. Radio Commun. PIMRC 2017*, Montreal, QC, Canada, 2017 (DOI: 10.1109/PIMRC.2017.8292777).

[33] A. Jamoos and M. Hussein, "Estimation of UFMC time-varying fading channel using adaptive filters", in *Proc. of the IEEE Int. Conf. on Promis. Electron. Technol. ICPET 2018*, Deir El-Balah, Palestinian Authority, 2018, pp. 43–48 (DOI: 10.1109/ICPET.2018.00014).

[34] A. Jamoos, E. Grivel, N. Shakarneh, and H. A. Nour, "Dual optimal filters for parameter estimation of a multivariate AR process from noisy observations", *IET Signal Process.*, vol. 5, no. 5, pp. 471–479, 2011 (DOI: 10.1049/iet-spr.2010.0066).

[35] J. G. Sekar and S. Sankarappan, "Enhanced channel estimation and performance analysis using H-infinity filter for MIMO-orthogonal frequency division multiplexing systems", *J. of Comp. Sci.*, vol. 11, no. 2, pp. 400–405, 2015 (DOI: 10.3844/jcssp.2015.400.405).

[36] B. Belgacem and S. Lamir, "Optimal distributed power control in wireless cellular network based on mixed Kalman/H_∞ filtering", AEU – Int. J. of Electron. and Commun., vol. 90, pp. 103–109, 2018 (DOI: 10.1016/j.aeue.2018.04.016).

[37] A. Jamoos, E. Grivel, N. Christov, and M. Najim, "Estimation of autoregressive fading channels based on two cross-coupled H_∞ filters", *Signal, Image and Video Process. J.*, vol. 3, no. 3, pp. 209–216, 2009 (DOI: 10.1007/s11760-008-0096-x).

[38] A. Jamoos, A. Abdo, H. A. Nour, and E. Grivel, "Two cross-coupled H_∞ filters for fading channel estimation in OFDM systems", in *Novel Algorithms and Techniques in Telecommunications and Networking*, Tarek Sobh, Khaled Elleithy, and Ausif Mahmood, Eds. Dordrecht: Springer, 2010, pp. 349–353 (DOI: 10.1007/978-90-481-3662-9_60).

[39] G. Bochechka, V. Tikhvinskiy, I. Vorozhishchev, A. Aitmagambetov, and B. Nurgozhin, "Comparative analysis of UFMC technology in 5G networks", in *Proc. Int. Siberian Conf. on Control and Commun. SIBCON 2017*, Astana, Kazakhstan, 2017 (DOI: 10.1109/SIBCON.2017.7998465).

[40] K. E. Baddour and N. C. Beaulieu, "Autoregressive modeling for fading channel simulation", *IEEE Trans. on Wirel. Commun.*, vol. 4, no. 4, pp. 1650–1662, 2005 (DOI: 10.1109/TWC.2005.850327).

[41] A. H. El Husseini, L. Ros, and E. P. Simon, "Second-order autoregressive model-based Kalman filter for the estimation of a slow fading channel described by the Clarke model: Optimal tuning and interpretation", *Elsevier Digit. Signal Process.*, vol. 90, pp. 125–141, 2019 (DOI: 10.1016/j.dsp.2019.04.008).

Ali Jamoos received his B.Sc. degree in Electronic Engineering from Al-Quds University, Jerusalem, in 1996; M.Sc. in Electronics and Communications from JUST University, Jordan, in 2000, and Ph.D. in Signal Processing and Communications from Bordeaux University, France, in 2007. His research interests are in the field of signal processing for wireless communications with a focus on mobile fading channel modeling, estimation and equalization, cellular network planning and optimization, OFDM- and CDMA-based mobile communication systems, as well as spectrum sensing for cognitive radio. He has published more than 30 research papers. He is an IEEE senior member. Currently, he is an Associate Professor at the Department of Electronic and Communication Engineering, Al-Quds University, Jerusalem, Palestine.

https://orcid.org/0000-0003-1605-7346
E-mail: ali.jamoos@staff.alquds.edu
Department of Electronic and Communication Engineering
Al-Quds University
Jerusalem, Palestine